Resonance-Free Low-Pass Filters for the AC Josephson Voltage Standard

Michio Watanabe, Paul D. Dresselhaus, and Samuel P. Benz, *Senior Member, IEEE*

***Abstract*—We have designed and characterized superconducting integrated circuits for the ac Josephson voltage standard that demonstrate significantly improved performance. The typical circuit consists of an array of superconductor–normal metal–superconductor Josephson junctions, which are placed in a transmission line and biased with a broad-band (dc-to-15 GHz) pulse-drive waveform. Additional low-speed (dc and audio frequency) bias and output leads contain on-chip inductors that act as low-pass filters. The operating margins of the array were improved by adding resistive shunts across these inductors to damp their intrinsic resonances. These resonances had previously degraded the integrity of the broad-band signal driving the array. We present simulations and measurements of these improved circuits that demonstrate no resonances in the range of 0.1–20 GHz. Moreover, the operating margins of the ac Josephson voltage standard were improved.**

***Index Terms*—Digital–analog conversion, Josephson arrays, microwave circuits, quantization, signal synthesis, standards, superconductor–normal–superconductor devices, voltage.**

I. Introduction

JOSEPHSON junctions have proven to be the basis for all dc voltage standards over the past 20 years [1], [2], by using the constant-voltage steps that appear in the dc current–voltage (I–V) characteristics [3]. Series arrays of several thousand Josephson junctions produce dc voltages up to 10 V. Accurate arbitrary waveforms and ac voltages have also been synthesized with Josephson junction arrays by use of digital-to-analog conversion techniques to generate programmable sequences of perfectly quantized Josephson pulses [4], [5]. Unlike the dc devices, the ac Josephson devices need broad-band response, dc to 15 GHz, since the drive is no longer a continuous sine wave.

In order to drive the junctions with broad-band pulse waveforms at microwave frequencies, the junctions are fabricated along the center conductor of a coplanar waveguide. It is also necessary to connect dc leads to the junctions to allow measurement of voltage across the junctions. Low-pass filters are required on these leads to prevent high-speed signal components from leaving the transmission line and reducing or modifying the broad-band bias signal that drives the array. We typically use a series of on-chip superconducting spiral inductors as the low-pass filters. Unfortunately, the intrinsic capacitance of these inductors causes resonances that are in the band of the broad-band drive signal. The resonances are usually not detrimental for dc voltage standard circuits that are biased at a single microwave frequency, provided that the drive frequency is chosen away from the resonances. The ac Josephson voltage standard being developed at NIST is driven with a digital bitstream that is clocked by 10-Gb/s pulses in combination with a 15-GHz continuous microwave drive for bipolar pulse operation [4], [6]. Using this technique, the NIST ac Josephson system has demonstrated precision arbitrary waveforms at audio frequencies with peak voltages up to 0.25 V [7]. To further improve the performance of the ac standard and achieve higher output voltages, it is crucial to have well-engineered on-chip low-pass filters and to eliminate the resonances in the frequency range from 0.1 to 20 GHz.

In this paper, we present new filters that show improved performance. Measurements of the frequency dependence of constant-voltage steps of previous circuit designs showed that resonances reduced the current range of these steps at a number of frequencies above 1 GHz. Simulations showed that these resonances were due to the on-chip inductors and that they could be damped by resistively shunting the inductors. We fabricated Josephson-junction circuits with these shunted-inductor low-pass filters, and confirmed the improved performance in the frequency dependence of the constant-voltage steps. A corresponding performance improvement was also observed in the pulse-driven ac standard.

II. Simulation

The circuit for the ac Josephson voltage standard is shown schematically in Fig. 1. The Josephson junctions are placed in a coplanar transmission line that is connected via a coaxial cable to the pulse and microwave sources, which in Fig. 1 are represented by the voltage source V_s. The voltage source has an output impedance of 50 Ω and the transmission line is terminated by an on-chip resistor $R_t = 50\ \Omega$. The low-pass filters, represented by LPF in Fig. 1, are used for measuring the low-frequency output voltage across the array and also for injecting an additional low-frequency bias to the Josephson array. The filters consist of a series of superconducting spiral inductors, and in some designs, each inductor is resistively shunted. Two leads are attached to the measurement side of each filter, for a low-frequency four-point measurement of the junctions.

Ideally, a low-pass filter would have a large inductance and no parasitic capacitances. However, real inductors have capacitance between overlaps, turn-to-turn capacitance, and

Manuscript received September 20, 2005; revised November 29, 2005. This paper was recommended by Associate Editor O. Mukhanov. The work of M. Watanabe was supported by the Postdoctoral Fellowships for Research Abroad from the Japan Society for the Promotion of Science (JSPS).

M. Watanabe is with the National Institute of Standards and Technology (NIST), Boulder, CO 80305 USA, and also with Frontier Research System, RIKEN, Wako, Saitama 351-0198, Japan (e-mail: michio@riken.jp).

P. D. Dresselhaus and S. P. Benz are with the National Institute of Standards and Technology (NIST), Boulder, CO 80305 USA (e-mail: haus@boulder.nist.gov).

Digital Object Identifier 10.1109/TASC.2005.863533

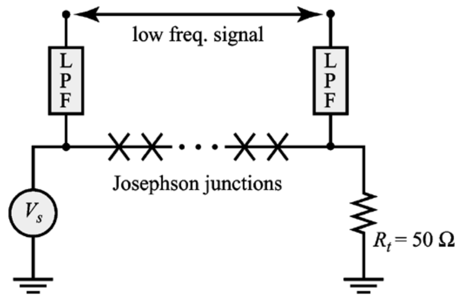

Fig. 1. Schematic diagram of the Josephson voltage standard. V_s represents the combined broad-band pulse and microwave source, and LPF represents the on-chip low-pass filter.

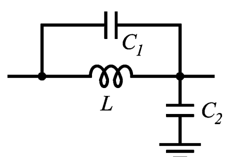

Fig. 2. Simple model of the spiral inductor showing the parasitic capacitances.

self-capacitance—all of which degrade the high-frequency performance of the filter. In our circuit simulations, the spiral inductor is modeled as shown in Fig. 2, where the parallel capacitance C_1 and the parasitic capacitance C_2 are considered in addition to the inductance L. In the simulations, the circuit is open after LPFs, i.e., neither the low-frequency leads that run up the cryoprobe nor the measurement apparatus connected to the leads are considered, because they have much larger inductance than the spiral inductors, and thus, do not produce resonances in the frequency range of interest, 0.1–20 GHz. For simplicity, the Josephson junctions are modeled as lumped-element 0.1-Ω resistors, which should be a good approximation for these frequencies. We used a SPICE-based simulator for these calculations.[1]

In general, resonances may be damped by shunting elements with resistors. Three possible damping configurations are shown in Fig. 3. The configuration shown in Fig. 3(b), in which the resistor is in series with the inductor, does not preserve zero dc resistance for our output voltage measurement, so this configuration was not chosen. Simulations and experiments of the shunt resistor that is capacitively coupled to ground, as in Fig. 3(c), confirm that it also effectively damps the resonances. Although, unlike Fig. 3(b), the filter resistance in Fig. 3(c) is still zero, it has the drawback that the capacitively shunted resistor may become leaky due to fabrication errors. For these reasons, we concentrate our discussion in this paper on the shunt configuration shown in Fig. 3(a), where a resistor simply shunts each spiral coil inductor.

Before using resistive shunts, we optimized circuit performance by using a low-pass filter consisting of six identical series inductors, thus minimizing the number of resonance frequencies. Fig. 4(a) shows the simulated ac current flowing though the Josephson junctions as a function of the frequency for this structure, each with (dashed) and without resistive shunts. The ac current is normalized to the dc value. In Fig. 4(a), each filter has six identical inductors with $L = 6$ nH, $C_1 = 0.15$ pF,

[1]http://www.linear.com/company/software.jsp

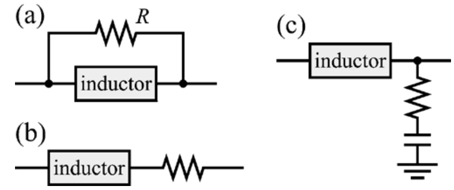

Fig. 3. Possible configurations for damping the resonances with a resistor.

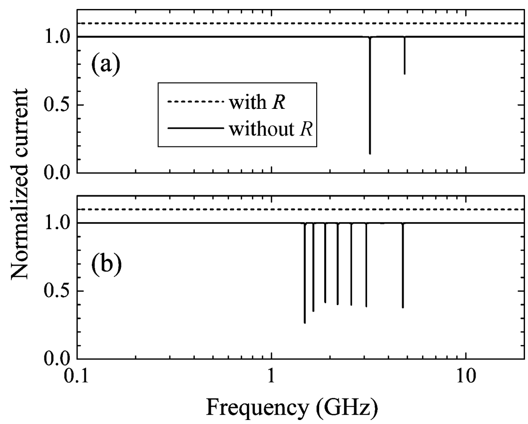

Fig. 4. Simulated ac current through the Josephson junctions in Fig. 1. Each filter has either (a) six identical or (b) eight cascaded series inductors. Both in (a) and (b), the inductors are resistively shunted in the dashed upper trace only. For clarity, the origin of the upper trace is shifted upwards by 0.1.

and $C_2 = 15$ fF. In the solid trace, the inductors are not resistively shunted, while in the upper dashed trace each inductor is shunted by $R = 50\ \Omega$. The origin of each upper trace is offset for clarity. Thus, the two traces are similar except for the resonant dips, showing that the resonances are eliminated by the resistive shunts.

In order to improve our circuit performance, we wished to decrease the cutoff frequency of our filters by increasing the total on-chip inductance. That is the reason we used six identical series coils for the data shown in Fig. 4(a). To further increase the inductance, we also investigated filters of series inductors with increasing values of inductance. We had hoped that cascading several small inductors would be better than having one large inductor because the capacitance for each inductor would be smaller, driving the resonance to higher frequency such that it is no longer in the bandwidth of the drive signal. Furthermore, we expected that the small coils at the beginning of the chain would cut off higher frequency signals that may resonate in larger coils further down the chain.

Through many experimental circuit designs, we found that more resonances appeared when the inductors are not identical, because coils of different sizes added different resonance frequencies. Our observation that resonances are more abundant with many nonidentical inductors is confirmed by our simulations, as shown in the solid trace of Fig. 4(b). The lower trace of Fig. 4(b), for eight different inductors with no shunt resistor ($L = 6$–25 nH, $C_1 = 0.15$–0.4 pF, and $C_2 = 15$–23 fF), has more resonances than the six identical coils in the lower trace of Fig. 4(a).

Fortunately, the resonances in the lower trace of Fig. 4(b) are also eliminated by resistively shunting the inductors. The circuit for the upper dashed trace of Fig. 4(b) (again offset for clarity) is

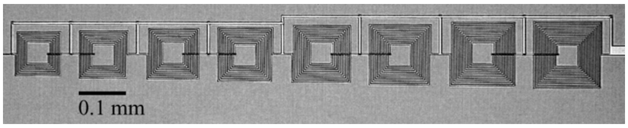

Fig. 5. Photograph of an on-chip low-pass filter (Type 3). Each Nb spiral inductor is shunted by a PdAu resistor.

the same as the lower trace except that each inductor is shunted by a range of resistances ($R = 50 - 91\ \Omega$). The resonances are clearly removed in the upper trace by the shunt resistors. We will show in Section IV that the simulation reproduces the behavior of the actual circuit reasonably well.

III. Experiment

We fabricated arrays of superconducting Josephson junctions on oxidized Si wafers of 76 mm (3 in) diameter using standard photolithography [8]. The junctions used in this experiment were $\mathrm{Nb/MoSi_2/Nb/MoSi_2/Nb}$, double-stacked superconductor–normal metal–superconductor (SNS) junctions [9]. Each array has 1280 stacks $\times$ 2 junctions per stack $= 2560$ junctions. The size of the junctions was $4 \times 8\ \mu\mathrm{m}^2$ and the thickness of their barriers was nominally 22 nm.

We characterized the junctions at 4 K by immersing the resulting $1 \times 1\ \mathrm{cm}^2$ chips in liquid He using a cryoprobe with spring fingers that electrically contact the chip. For the junction arrays reported in this paper, we obtained $I_c = 11.5 \pm 0.5$ mA and $R_n = 4.0 \pm 0.1\ \mathrm{m}\Omega$, where I_c is the critical current and R_n is the normal resistance per junction. The characteristic voltage of $I_c R_n = 46\ \mu\mathrm{V}$, resulting from the 22-nm $\mathrm{MoSi_2}$ barrier, is consistent with the earlier results [10].

Concerning the filter designs, we report the following three types: six identical inductors in series with no shunt resistor (Type 1), six identical inductors, as in Type 1, except each inductor is shunted with a 50-Ω resistor (Type 2), and eight cascaded inductors with increasing inductance and with each inductor having a separate shunt resistor with values from 50 to 91 Ω (Type 3, see Fig. 5 for a photograph). Type 1 is the conventional NIST design used in previous ac work. The values of L, C_1, and C_2 used in Fig. 4(a) are the estimates for Types 1 and 2, and those in Fig. 4(b) are for Type 3. For the estimate of the coil inductors, we used an online inductance calculator[2] that is based on [11].

For testing purposes, Josephson arrays were driven with a continuous-wave microwave source. For frequencies above 8 GHz, a microwave amplifier was used to produce sufficient amplitude to suppress the zero-voltage step.

IV. Results and Discussion

Typical I–V characteristics of the Josephson arrays are shown in Fig. 6. The I–V curve shows constant-voltage Shapiro steps when the junctions are driven with microwave bias. The steps are at integer multiples of $V = Nf/K_J = 79.405$ mV for the number of junctions $N = 2560$ and the $f = 15$ GHz drive frequency.

[2]http://smirc.stanford.edu/spiralCalc.html

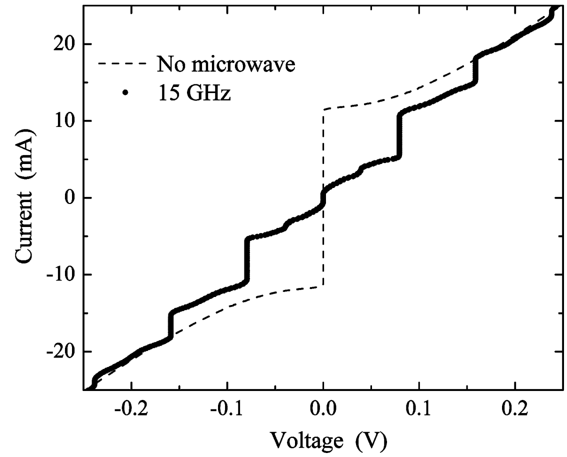

Fig. 6. I–V characteristics of an array of 2560 SNS Josephson junctions with and without microwave irradiation.

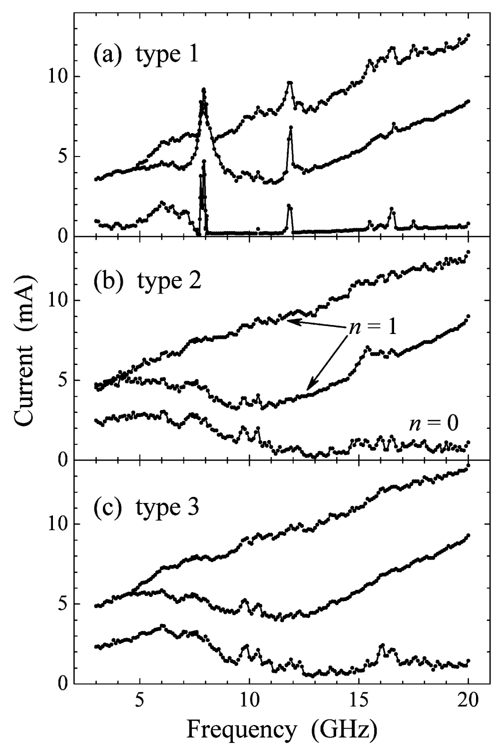

Fig. 7. Frequency dependence of the $n = 0$ and $n = 1$ Shapiro steps for $N = 2560$ Josephson-junction arrays. In each frame, the bottom trace shows the $n = 0$ step, whereas the other traces denote the lower and upper limits of the $n = 1$ step. To maximize the $n = 1$ step, the microwave power was monotonically increased with frequency so as to compensate for the loss in the coaxial cable and connections, as well as for the junction dynamical properties. A microwave amplifier was used above 8 GHz, but not at low frequencies.

Shapiro steps were measured over a broad frequency range in order to characterize the on-chip low-pass filters. As the microwave source was stepped in frequency, the limits of the $n = 0$ and $n = 1$ Shapiro steps were measured and plotted as in Fig. 7. This method of characterization has been previously employed at NIST [12] to characterize operating margins of the ac Josephson voltage standard. Note that a measurable $n = 1$ step appears in all three plots for frequencies above about 5 GHz. In Type 1 [Fig. 7(a)], however, the $n = 1$ step

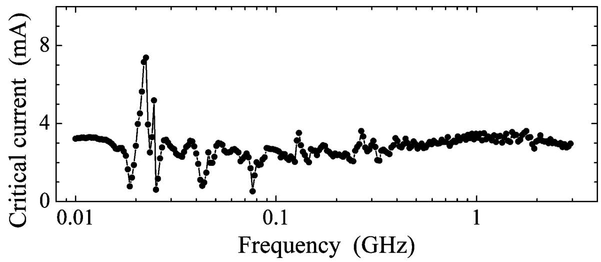

Fig. 8. Frequency dependence of the critical current ($n = 0$ Shapiro step) for Type 3. The microwave power was monotonically increased with frequency so that the critical current becomes about 3 mA on average. No microwave amplifier was used.

disappears around 8 GHz, and is also significantly smaller near 12 and 16.5 GHz. These resonances have been common to many NIST designs [12], and indicate that there is some deviation from the designed microwave distribution at these frequencies, which is unfavorable for the ac voltage standard. Because the $n = 0$ step increases at the same time, the data suggest that much lower microwave power is reaching the array, and that the microwave bias that does reach the array has a poor distribution across the array, leading to smaller $n = 1$ steps. These features can be qualitatively related to the dips in the simulation of Fig. 4(a). The features in Fig. 7(a) are not as sharp as the dips in Fig. 4(a); however, this difference would be reasonable when we note that in actual circuits there should be dissipation mechanisms, such as coupling to the environment, which will broaden the resonances. More importantly, the features are eliminated by resistively shunting each on-chip spiral inductor, as shown in Fig. 7(b). The circuits for Figs. 7(a) and (b) were fabricated on the central region of the same wafer, and the features in question were observed for multiple Type 1 chips, as were the expected absence of these resonances for multiple Type 2 chips. The circuits for Fig. 7(c) were fabricated at the same time as well, but on a different wafer; however, this wafer also had the designs for Fig. 7(a), which showed similar results. Thus, the difference between Figs. 7(a) and (b) is due solely to the shunt resistors. Furthermore, the traces in Fig. 7(c) for the cascaded series of shunted inductors are apparently resonance free, like the behavior shown in Fig. 7(b), indicating that the shunt resistors are also effective for the case in which the filters have a number of inductors with a range of values.

We have also confirmed by measuring the critical current ($n = 0$ Shapiro step) that in all three types there are no large resonances at lower frequencies (down to 0.1 GHz). An example of this measurement is shown in Fig. 8 for a series of shunted inductors as in Fig. 7(c). Down to 0.1 GHz, the curve is relatively featureless. There are probe-related resonances below 0.1 GHz, but fortunately, the frequencies of the resonances are low enough that there is little impact on the operating margin of the ac Josephson voltage standard.

On previous ac Josephson circuits, the number of taps per array was limited, because the additional associated resonances severely degraded the operating margins [6]. When two taps were put on each side of the Josephson array, which is necessary for true four-point ac measurements, no operating margins were obtained. However, using the shunted filters, we have been able to obtain appreciable operating margins even for circuits with four separately filtered taps across the Josephson array. This has allowed the first metrological ac measurements to be made using Josephson arrays.

V. Conclusion

Based on the circuit simulations, we have designed and characterized on-chip low-pass filters for ac Josephson voltage standards. The filter consists of a series of spiral inductors, in which each inductor is resistively shunted. We have confirmed that the shunted-coil filters indeed produce no resonances at frequencies between 0.1 and 20 GHz, as predicted by the simulations. Using these filters, we have achieved improved operating margins of the ac Josephson voltage standard and the first true four-point ac Josephson measurements.

Acknowledgment

The authors would like to thank N. Hadacek and C. J. Burroughs for instrumentation and measurement assistance, and Y. Chong for fabrication assistance.

References

[1] R. L. Kautz, "Design and operation of series-array Josephson voltage standards," in *Metrology at the Frontiers of Physics and Technology*, L. Crovini and T. J. Quinn, Eds. Amsterdam, The Netherlands: Elsevier, 1992, pp. 259–296.

[2] C. A. Hamilton, "Josephson voltage standards," *Rev. Sci. Instrum.*, vol. 71, no. 10, pp. 3611–3623, Oct. 2000.

[3] S. Shapiro, "Josephson currents in superconducting tunneling: the effect of microwaves and other observations," *Phys. Rev. Lett.*, vol. 11, no. 2, pp. 80–82, Jul. 1963.

[4] S. P. Benz and C. A. Hamilton, "A pulse-driven programmable Josephson voltage standard," *Appl. Phys. Lett.*, vol. 68, no. 22, pp. 3171–3173, May 1996.

[5] O. A. Chevtchenko, H. E. van den Brom, E. Houtzager, R. Behr, J. Kohlmann, J. M. Williams, T. J. B. M. Janssen, L. Palafox, D. A. Humphereys, F. Piquemal, S. Djordjevic, O. Monnoye, A. Poletaeff, R. Lapuh, K.-E. Rydler, and G. Eklund, "Realization of a quantum standard for ac voltage' overview of a European research project," *IEEE Trans. Instrum. Meas.*, vol. 54, no. 2, pp. 628–631, Apr. 2005.

[6] S. P. Benz, C. A. Hamilton, C. J. Burroughs Jr., and T. E. Harvey, "AC and dc bipolar voltage source using quantized pulses," *IEEE Trans. Instrum. Meas.*, vol. 48, no. 2, pp. 266–269, Apr. 1999.

[7] S. P. Benz and C. A. Hamilton, "Application of the Josephson effect to voltage metrology," *Proc. IEEE*, vol. 92, no. 10, pp. 1617–1629, Oct. 2004.

[8] Y. Chong, P. D. Dresselhaus, and S. P. Benz, "Electrical properties of Nb–$MoSi_2$–Nb Josephson junctions," *Appl. Phys. Lett.*, vol. 86, no. 23, p. 232505, Jun. 2005.

[9] P. D. Dresselhaus, Y. Chong, J. H. Plantenberg, and S. P. Benz, "Stacked SNS Josephson junction arrays for quantum voltage standards," *IEEE Trans. Appl. Supercond.*, vol. 13, no. 2, pp. 930–933, Jun. 2003.

[10] Y. Chong, P. D. Dresselhaus, S. P. Benz, and J. E. Bonevich, "Effects of interlayer electrode thickness in $Nb/(MoSi_2/Nb)_N$ stacked Josephson junctions," *Appl. Phys. Lett.*, vol. 82, no. 15, pp. 2467–2469, Apr. 2003.

[11] S. S. Mohan, M. del Mar Hershenson, S. P. Boyd, and T. H. Lee, "Simple accurate expressions for planar spiral inductances," *IEEE J. Solid-State Circuits*, vol. 34, no. 10, pp. 1419–1424, Oct. 1999.

[12] P. D. Dresselhaus, Y. Chong, and S. P. Benz, "Stacked Nb–$MoSi_2$–Nb Josephson junctions for ac voltage standards," *IEEE Trans. Appl. Supercond.*, vol. 15, no. 2, pp. 449–452, Jun. 2005.

Michio Watanabe was born in Akita, Japan, on October 6, 1971. He received the B.S., M.S., and Dr. of Science degrees in physics from the University of Tokyo, Japan, in 1994, 1996, and 1999, respectively.

He was a Postdoctoral Fellow (1999–2001) of the Japan Society for the Promotion of Science (JSPS), and with Keio University, Japan and the Royal Institute of Technology (KTH), Sweden. Then, he was with RIKEN, Japan as a Special Postdoctoral Researcher (2001–2003). Since 2003, he has been supported by the JSPS Postdoctoral Fellowships for Research Abroad, and with the National Institute of Standards and Technology (NIST), Boulder, CO, as a Guest Researcher. He has also been with Frontier Research System, RIKEN as a researcher. He has worked on the quantum phase transitions in disordered electronic systems, experimental techniques at very low temperatures, and fabrication and characterization of nanometer- and micrometer-scale electronic circuits.

Dr. Watanabe is a member of the Physical Society of Japan, the Royal and Ancient Polar Bear Society, and the American Physical Society.

Paul D. Dresselhaus was born on January 5, 1963, in Arlington, MA. He majored in both physics and electrical engineering at MIT in 1985, and received the Ph.D. degree in applied physics from Yale University, New Haven, CT, in 1991.

In 1999, Dr. Dresselhaus joined the Quantum Voltage Project at the National Institute of Standards and Technology (NIST), Boulder, CO, where he has developed novel superconducting circuits and broad-band bias electronics for precision voltage waveform synthesis and programmable voltage standard systems. For three years at Northrop Grumman, he designed and tested numerous gigahertz speed superconductive circuits, including code generators and analog-to-digital converters. He also upgraded the simulation and layout capabilities at Northrop Grumman to be among the world's best. His previous work as a Postdoctoral Assistant at SUNY Stony Brook focused on the nanolithographic fabrication and study of Nb–AlO_x–Nb junctions for single electron and SFQ applications, single electron transistors, and arrays in Al–AlO_x tunnel junctions, and the properties of ultrasmall Josephson junctions.

Samuel P. Benz (SM'00) was born in Dubuque, IA, on December 4, 1962. He majored in both physics and mathematics at Luther College, Decorah, IA, where he graduated *summa cum laude* with the B.A. degree in 1985. He was awarded an R.J. McElroy fellowship (1985–88) to pursue a Ph.D., and received the M.A. and Ph.D. degrees in physics from Harvard University, Cambridge, MA, in 1987 and 1990.

In 1990, he began working at the National Institute of Standards and Technology (NIST) as an NIST/NRC Postdoctoral Fellow and joined the permanent staff in January 1992. He has been Project Leader of the Quantum Voltage Project at NIST since October 1999. He has worked on a broad range of topics within the field of superconducting electronics, including Josephson junction array oscillators, single flux quantum logic, ac and dc Josephson voltage standards, and Josephson waveform synthesis. He has 105 publications, three patents in the field of superconducting electronics, and a U.S. Department of Commerce Gold Medal for Distinguished Achievement.

Dr. Benz is a member of Phi Beta Kappa and Sigma Pi Sigma